

Supplementary Information

Elucidating the Mechanism of Photochemical CO₂ Reduction to CO Using a Cyanide-Bridged Di-Manganese Complex

Kailyn Y. Cohen, Adam Reinhold, Rebecca Evans, Tia S. Lee, Hsin-Ya Kuo,
Delaan G. Nedd, Gregory D. Scholes, and Andrew B. Bocarsly*

Department of Chemistry, Frick Laboratory, Princeton University, Princeton, New Jersey, United States

*Email: bocarsly@princeton.edu

Contents

IR spectrum of s-Mn₂CN⁺ , [Mn(bpy)(CO) ₃ (MeCN)](PF ₆), and [Mn(bpy)(CO) ₃ (CN)]	S2
Gas phase IR spectrum of headspace of Mn₂CN⁺	S2
UV-vis and IR spectra of [Mn(bpy)(CO) ₃ (MeCN)] ⁺ under irradiation	S3
Liquid phase IR of Mn-Mn exposed to CO ₂	S4
UV-vis of Mn-Mn before and after exposure to CO ₂	S4
UV-vis of [Mn(bpy)(CO) ₃ Br] and CO ₂ under irradiation	S5
UV-vis of [Mn(bpy)(CO) ₃ (MeCN)] ⁺ and CO ₂ under irradiation	S5
³¹ P NMR of [Mn(bpy)(CO) ₃ (MeCN)] ⁺ and Mn-Mn with PPh ₃	S6
EPR spectrum of Mn-Mn exposed to CO ₂	S6
Gas phase IR spectrum of headspace of Mn-Mn before and after irradiation	S7
UV-vis of Mn₂CN⁺ irradiated under argon, then exposed to CO ₂	S7
¹ H NMR of [Mn(bpy)(CO) ₃ (MeCN)] ⁺ and [Mn(bpy)(CO) ₂ (MeCN) ₂] ⁺	S8
Quantum Yield Calculation	S8
IR shifts of common Mn and Re complexes	S9

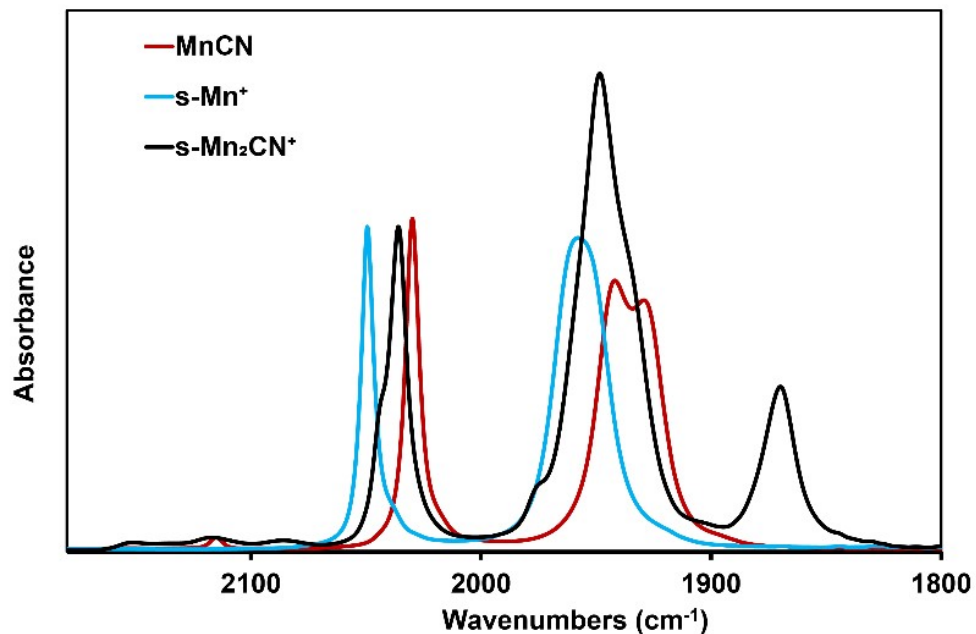


Figure S1. The liquid phase IR spectrum of $\text{s-Mn}_2\text{CN}^+$ compared with those of $[\text{Mn}(\text{bpy})(\text{CO})_3(\text{MeCN})](\text{PF}_6)$ (blue) and $[\text{Mn}(\text{bpy})(\text{CO})_3(\text{CN})]$ (red).

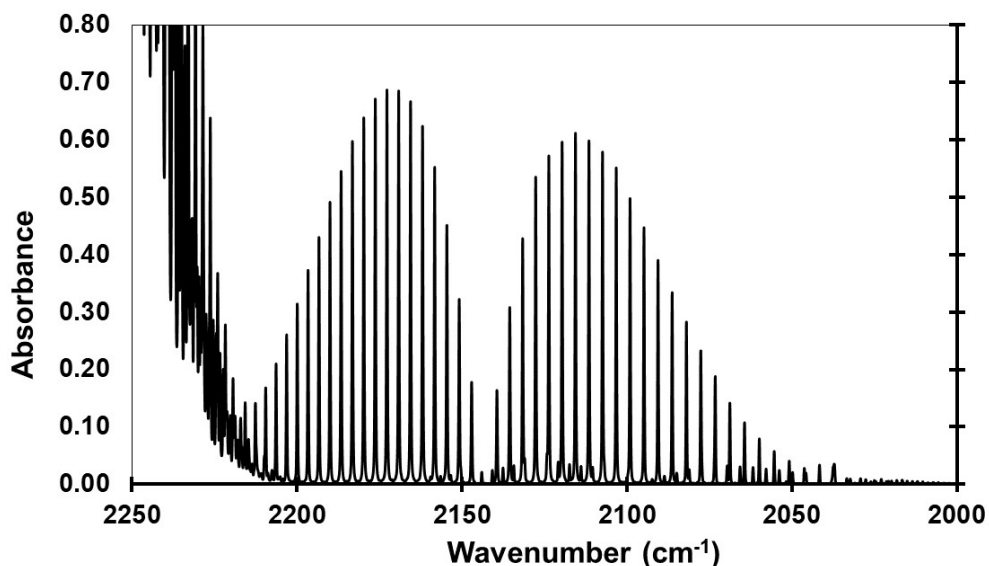


Figure S2. Headspace gas infrared spectrum of 1 mM Mn_2CN^+ with 1 M phenol after irradiation with 395 nm LED for 1 h. The ratio of $^{13}\text{CO}/^{12}\text{CO}$ is 5%.

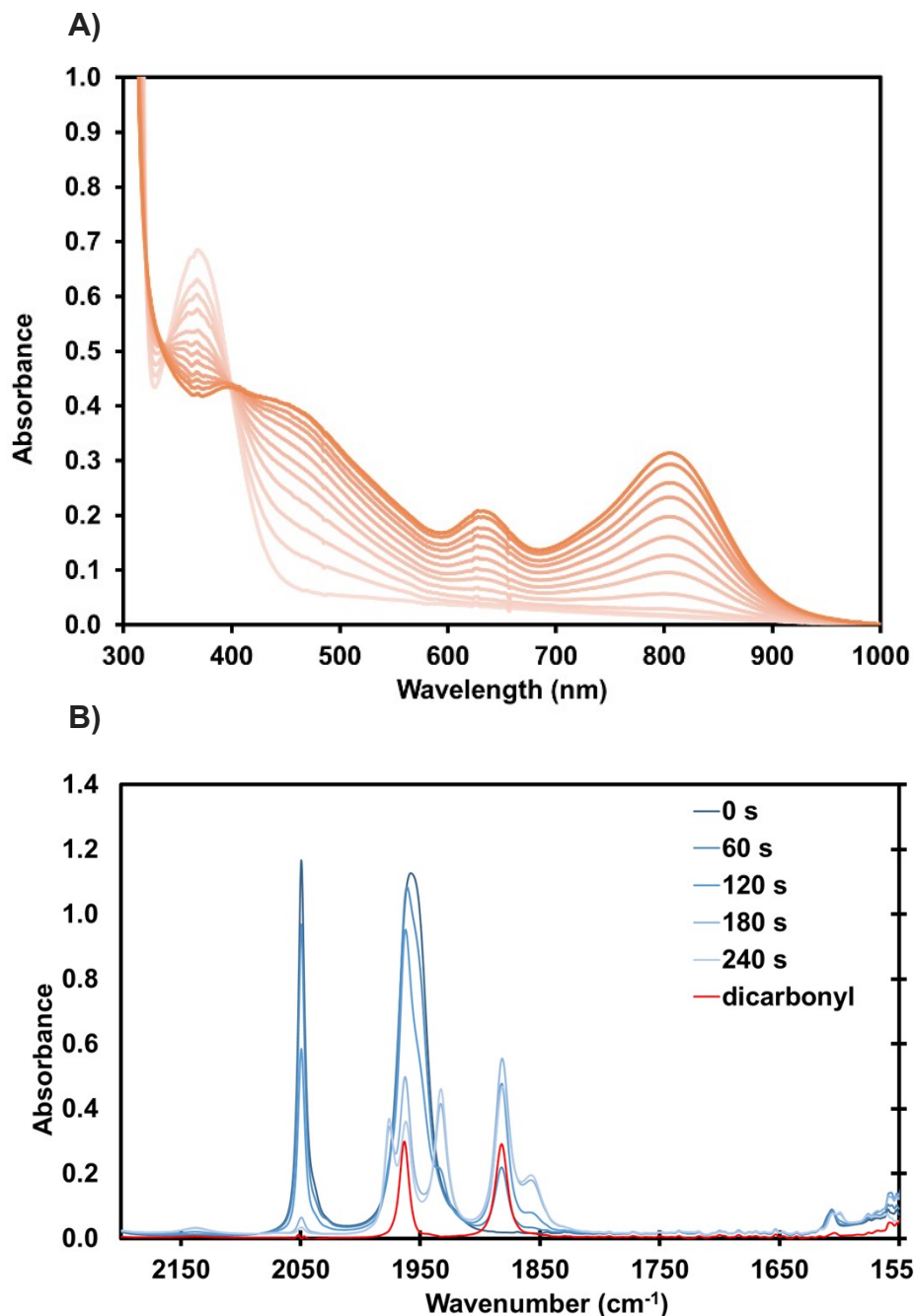


Figure S3. A) UV-vis spectra of 0.33 mM $[\text{Mn}(\text{bpy})(\text{CO})_3(\text{MeCN})]^+$ in degassed MeCN taken every 10 s of irradiation at 395 nm, showing a decrease in $[\text{Mn}(\text{bpy})(\text{CO})_3(\text{MeCN})]^+$ at 375 nm and an increase in the dicarbonyl species, $[\text{Mn}(\text{bpy})(\text{CO})_2(\text{MeCN})_2]^+$ (shoulder ~500 nm) for the first 20 s. From 30 to 110 s, **Mn-Mn** is detected. B) Liquid IR spectra of 10 mM $[\text{Mn}(\text{bpy})(\text{CO})_3(\text{MeCN})]^+$ in degassed MeCN, taken every 60 s of irradiation at 395 nm. The dicarbonyl signal (red) is the initial signal subtracted from the signal at 60 s, showing two peaks at 1960 and 1880 cm^{-1} .

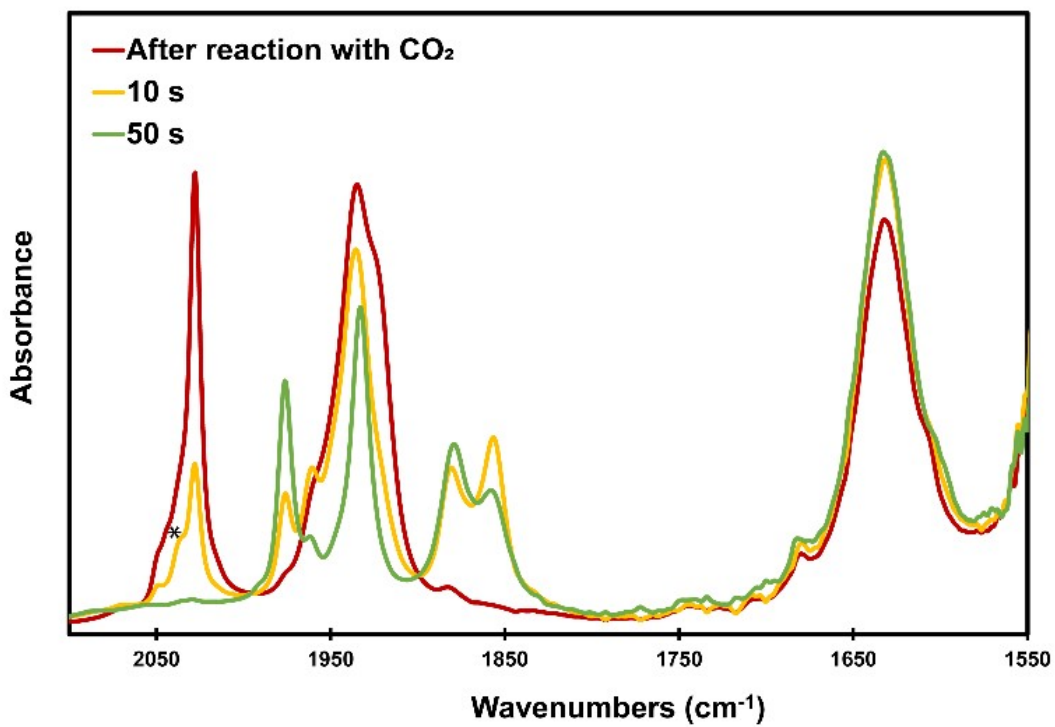


Figure S4. Liquid phase IR spectra immediately after **Mn-Mn** in degassed MeCN was combined with CO_2 -saturated MeCN in the dark (red), and then after irradiation with 395 nm light.
*indicates an axial carbonyl peak.

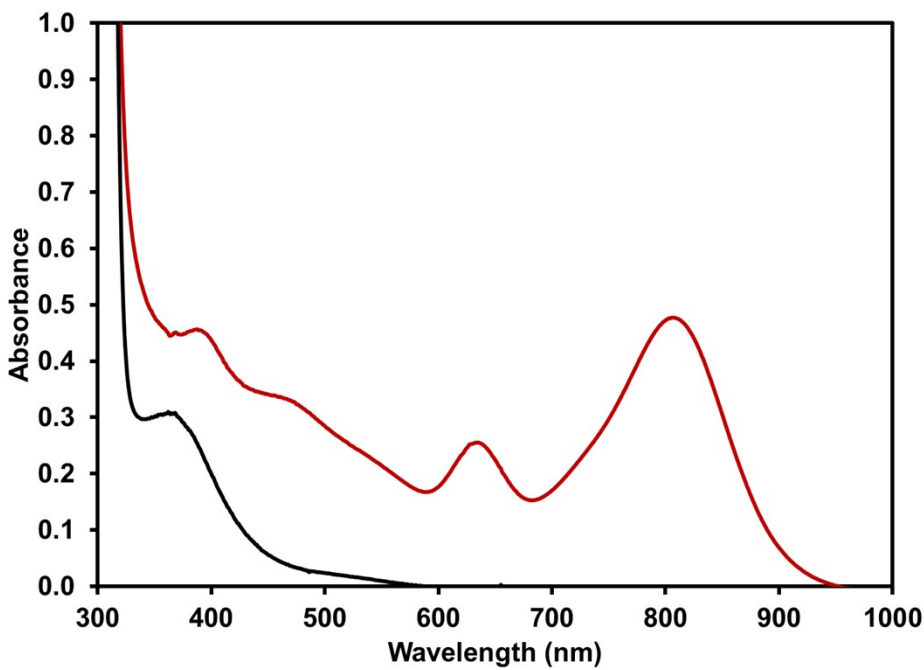


Figure S5. UV-vis of 0.04 mM **Mn-Mn** and 1 M PhOH in degassed MeCN (red). After the introduction of CO_2 , two peaks at 375 and a shoulder \sim 500 nm corresponding to $[\text{Mn}(\text{bpy})(\text{CO})_3(\text{MeCN})]^+$ and $[\text{Mn}(\text{bpy})(\text{CO})_2(\text{MeCN})_2]^+$, respectively, persist in solution.

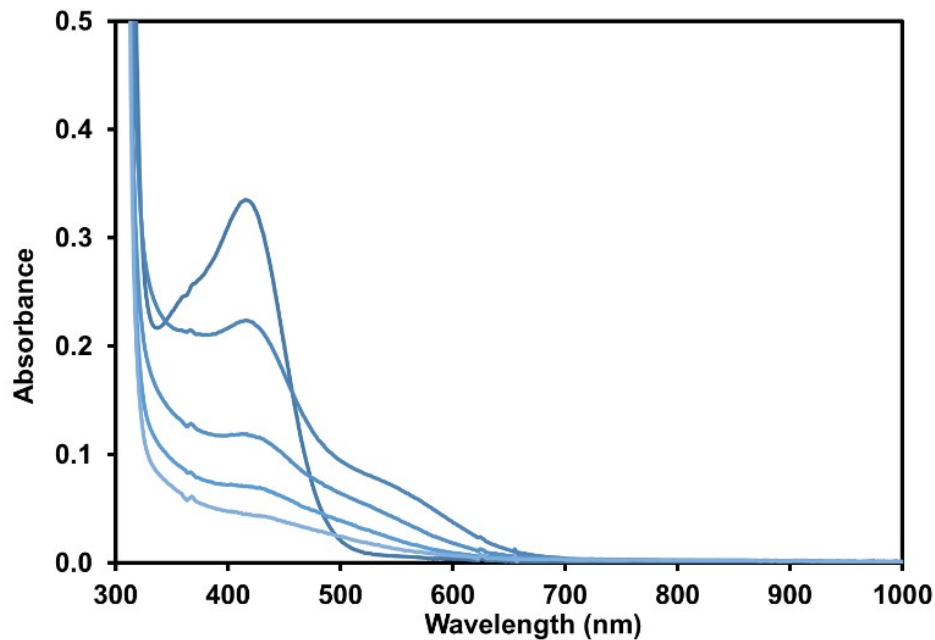


Figure S6. UV-vis of 0.087 mM $[\text{Mn}(\text{bpy})(\text{CO})_3\text{Br}]$ and 10 mM PhOH in CO_2 -saturated MeCN every 60 s of irradiation at 395 nm, showing a decrease in the *fac* isomer and an increase in the *mer* isomer (shoulder \sim 570 nm.) No **Mn-Mn** was detected.

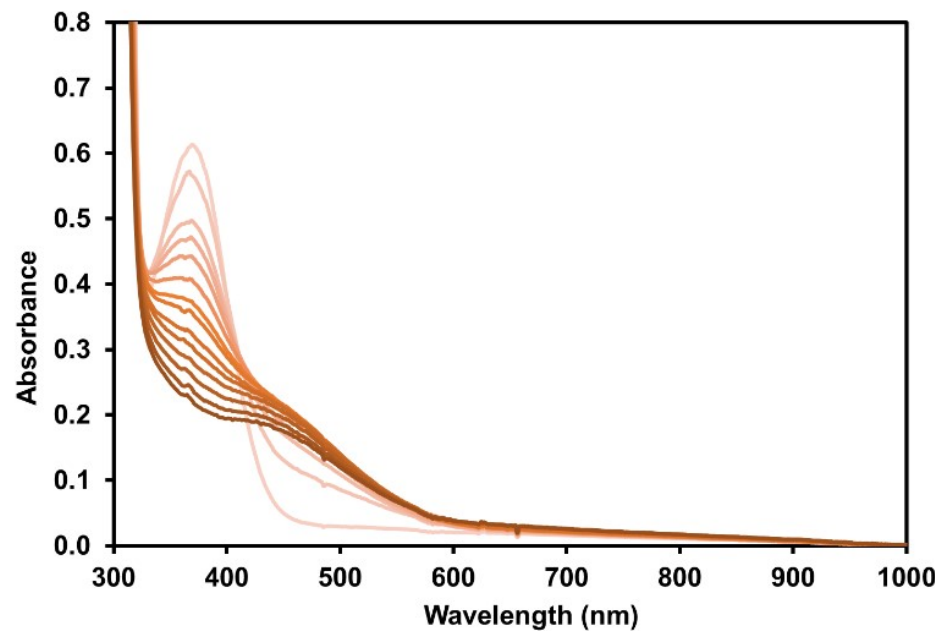


Figure S7. UV-vis of 0.33 mM $[\text{Mn}(\text{bpy})(\text{CO})_3(\text{MeCN})]^+$ in CO_2 -saturated MeCN every 10 s of irradiation at 395 nm, showing a decrease in $[\text{Mn}(\text{bpy})(\text{CO})_3(\text{MeCN})]^+$ at 375 nm and an increase in the dicarbonyl species, $[\text{Mn}(\text{bpy})(\text{CO})_2(\text{MeCN})_2]^+$ (shoulder \sim 500 nm). No **Mn-Mn** was detected.

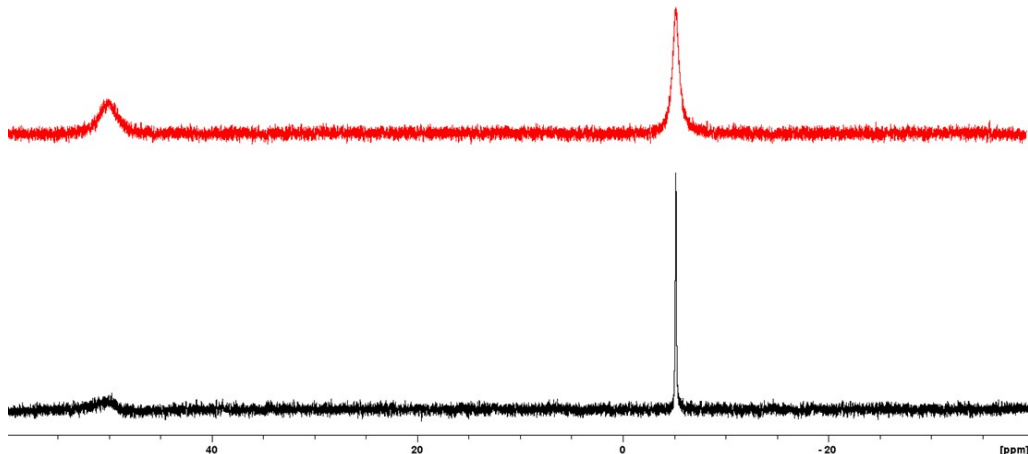


Figure S8. ^{31}P NMR of 15.26 mM PPh_3 and 14 mM $[\text{Mn}(\text{bpy})(\text{CO})_3(\text{MeCN})]^+$ (red) and 15.26 mM PPh_3 and 14 mM **Mn-Mn** (black). Free PPh_3 is located at -5.14 ppm and ligated PPh_3 is located at 49.75 ppm. ^{31}P NMR spectra were referenced to 85% H_3PO_4 solution as an external standard in d-MeCN.

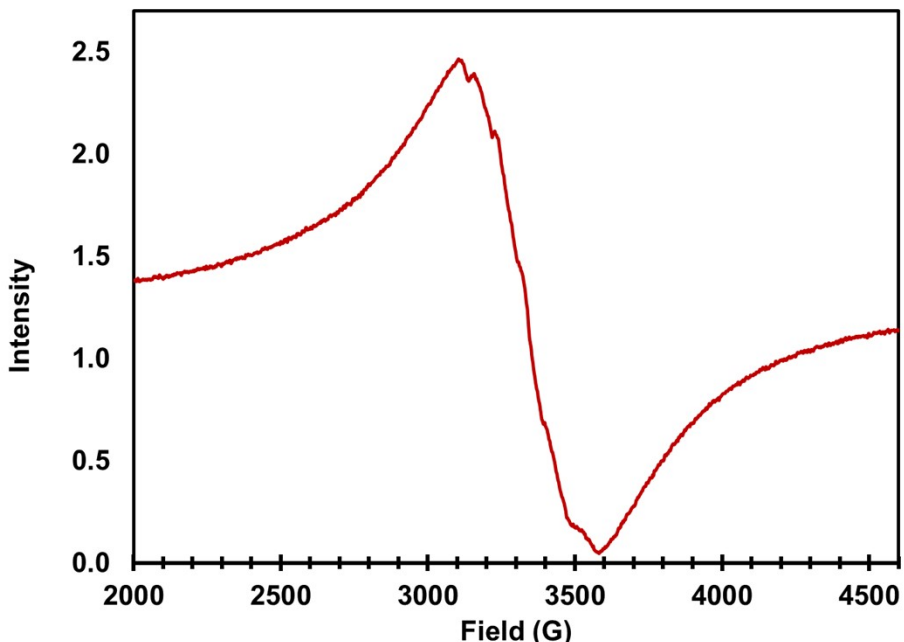


Figure S9. X-band EPR spectrum (10 K) of **Mn-Mn** in degassed MeCN upon addition of CO_2 in the dark, followed by freezing at 4 K. The EPR signal ($g = 2.001$) is indicative of a Mn^{II} species.

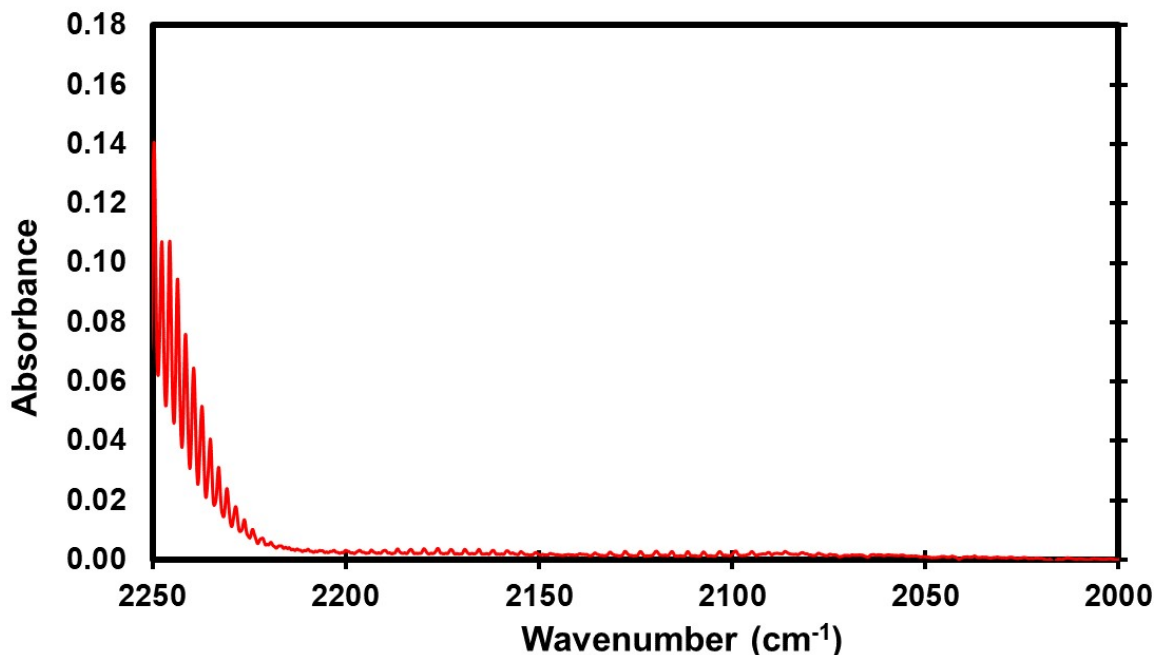


Figure S10. Headspace gas infrared spectra of ~6.5 mM Mn-Mn with 1 M phenol before irradiation with 395 nm LED for 3 h, showing no detectable CO in the headspace.

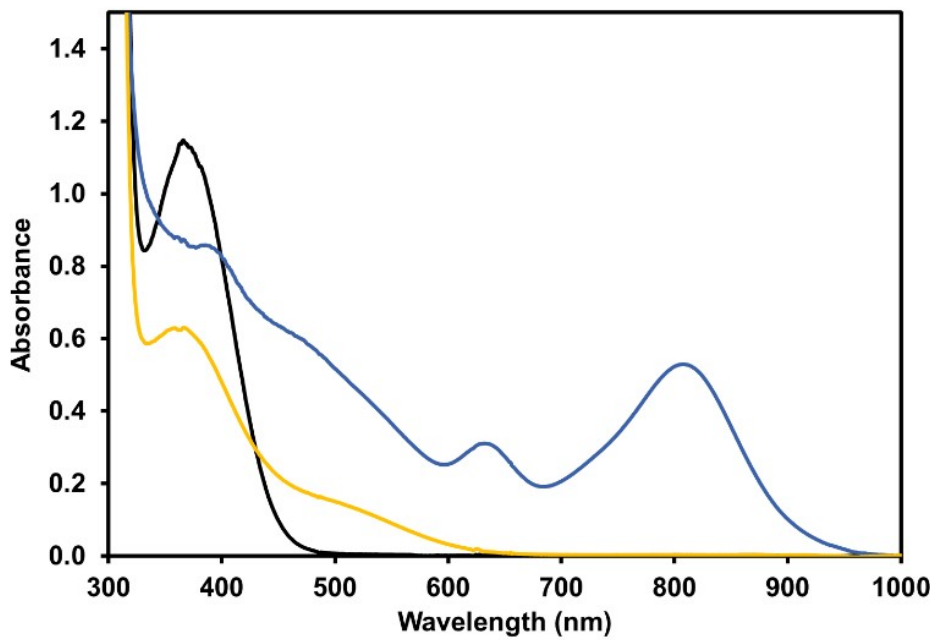


Figure S11. UV-vis of 0.1 mM Mn_2CN^+ and 1 M PhOH in degassed MeCN (yellow) after irradiation for 300 s at 395 nm (blue) showing Mn-Mn formation. After the introduction of CO_2 , two peaks at 375 and a shoulder ~500 nm corresponding to $[\text{Mn}(\text{bpy})(\text{CO})_3(\text{MeCN})]^+$ and $[\text{Mn}(\text{bpy})(\text{CO})_2(\text{MeCN})_2]^+$, respectively, persist in solution.

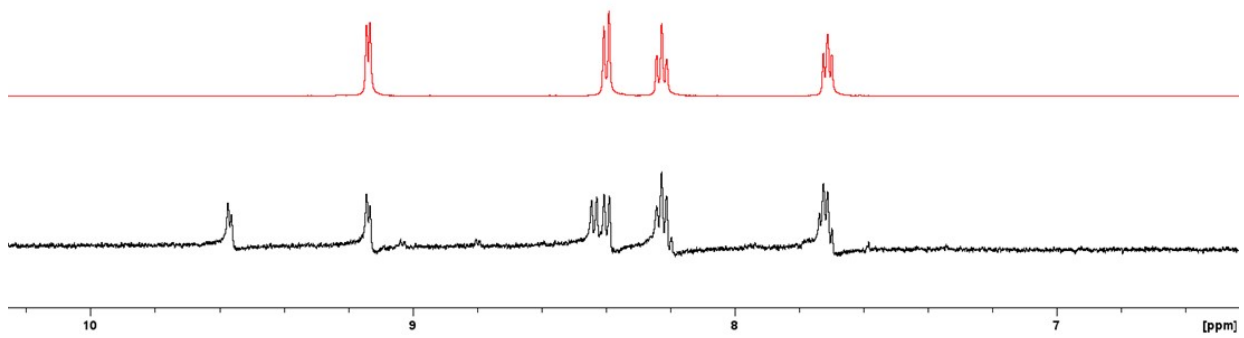


Figure S12. ^1H NMR of $[\text{Mn}(\text{bpy})(\text{CO})_3(\text{MeCN})]^+$ (red) and $[\text{Mn}(\text{bpy})(\text{CO})_2(\text{MeCN})_2]^+$ (black) in d-MeCN.

Quantum Yield Calculation:

$$\text{Quantum Yield} = \left(\frac{\text{mol CO}}{\text{(light absorbed, } W\text{)}(\text{irradiation time, } s)} \right) \text{ (energy per Einstein)}$$

$$0.64 = \left(\frac{4.98 \times 10^{-6} \text{ mol CO}}{\left(\frac{(0.00130 \text{ J/s})(1800 \text{ s})}{\left(\frac{hc}{395 \times 10^{-9} \text{ m}} \right) N_A} \right)} \right)$$

Intensity absorbed = 1.30 mW @ 395 nm

Energy per Einstein = $(hc/395 \text{ E -9 m}) * N_A$

N_A = Avogadro's number

Irradiation time = 1800 s

Table S1. IR shifts of common Mn and Re complexes

Mn Complex	CO stretches and OCO stretches denoted with * (cm^{-1}) exptl.	CO stretches (cm^{-1}) exptl. calc.	Solvent	Ref.
<i>fac</i> -Mn(bpy)(CO) ₃ CN	2030, 1941, 1934		MeCN	1
<i>fac</i> -Mn(bpy)(CO) ₃ Cl	2025, 1936, 1913		THF	2
<i>fac</i> -Mn(bpy)(CO) ₃ Br	2023, 1935, 1914		THF	3
<i>mer</i> -Mn(bpy)(CO) ₃ Br	2043, 1948, 1903		THF	3
<i>fac</i> -[Mn(bpy)(CO) ₃ (MeCN)] ⁺	2049, 1957		MeCN	4
[Mn(bpy)(CO) ₄] ⁺	2130, 2046, 2024, 1984		MeCN	4
[Mn ⁰ (mesbpy)(CO) ₃] [·]	1973, 1883, 1866		THF	5
<i>fac</i> -Mn ^I (bpy)(CO) ₃ (COOH)	2013; ~1650* and 1600*		MeCN	6
<i>fac</i> -Mn ^I (mesbpy)(CO) ₃ (COOH)	2007		THF	5
[Mn(bpy)(CO) ₂ (MeCN) ₂] ⁺	1961, 1883		MeCN	7
<i>fac</i> -Mn(bpy)(CO) ₃ H	1991, 1892, 1888		MeCN	8
[Mn(bpy)(CO) ₃] ₂	1976, 1931, 1880, 1860		2-MeTHF	9
[Mn(bpy)(CO) ₃] ₂ (μ-CN)	2152, 2043, 2035, 1946		MeCN	1
[Mn(bpy)(CO) ₃ -CN-Mn(bpy)(CO) ₃ (MeCN)] ⁺	2116, 2035, 1946, 1869	2125, ~2030, ~1940, 1870	MeCN	This work
<i>mer</i> -[Mn ^{II} (bpy)(CO) ₃ (COOH)] ⁺	2036, 1633*	2037, 2001, 1649	MeCN	This work

REFERENCES

1. Kuo, H.-Y.; S. Lee, T.; T. Chu, A.; E. Tignor, S.; D. Scholes, G.; B. Bocarsly, A., A cyanide-bridged di-manganese carbonyl complex that photochemically reduces CO₂ to CO. *Dalton Transactions* **2019**, 48 (4), 1226-1236.
2. Stor, G.; Stufkens, D.; Vernooijns, P.; Baerends, E.; Fraanje, J.; Goubitz, K., X-ray Structure of fac-IMn(CO)₃(bpy) and Electronic Structures and Transitions of the Complexes fac-XMn(CO)₃(bpy) (X= Cl, I) and mer-ClIMn(CO)₃(bpy). *Inorganic Chemistry* **1995**, 34 (6), 1588-1594.
3. Stor, G. J.; Morrison, S. L.; Stufkens, D. J.; Oskam, A., The Remarkable Photochemistry of fac-XMn(CO)₃(.α.-diimine) (X =Halide): Formation of Mn₂(CO)₆(.α.-diimine)₂ via the mer Isomer and Photocatalytic Substitution of X- in the Presence of PR₃. *Organometallics* **1994**, 13 (7), 2641-2650.
4. Kuo, H.-Y.; Tignor, S. E.; Lee, T. S.; Ni, D.; Park, J. E.; Scholes, G. D.; Bocarsly, A. B., Reduction-induced CO dissociation by a [Mn(bpy)(CO)₄][SbF₆] complex and its relevance in electrocatalytic CO₂ reduction. *Dalton Transactions* **2020**, 49 (3), 891-900.
5. Sampson, M. D.; Nguyen, A. D.; Grice, K. A.; Moore, C. E.; Rheingold, A. L.; Kubiak, C. P., Manganese Catalysts with Bulky Bipyridine Ligands for the Electrocatalytic Reduction of Carbon Dioxide: Eliminating Dimerization and Altering Catalysis. *Journal of the American Chemical Society* **2014**, 136 (14), 5460-5471.
6. Madsen, M. R.; Rønne, M. H.; Heuschen, M.; Golo, D.; Ahlquist, M. S. G.; Skrydstrup, T.; Pedersen, S. U.; Daasbjerg, K., Promoting Selective Generation of Formic Acid from CO₂ Using Mn(bpy)(CO)₃Br as Electrocatalyst and Triethylamine/Isopropanol as Additives. *Journal of the American Chemical Society* **2021**, 143 (48), 20491-20500.

7. Yempally, V.; Moncho, S.; Hasanayn, F.; Fan, W. Y.; Brothers, E. N.; Bengali, A. A., Ancillary Ligand Effects upon the Photochemistry of $\text{Mn}(\text{bpy})(\text{CO})_3\text{X}$ Complexes ($\text{X} = \text{Br}^-$, PhCC^-). *Inorganic Chemistry* **2017**, *56* (18), 11244-11253.
8. Franco, F.; Cometto, C.; Nencini, L.; Barolo, C.; Sordello, F.; Minero, C.; Fiedler, J.; Robert, M.; Gobetto, R.; Nervi, C., Local Proton Source in Electrocatalytic CO_2 Reduction with $[\text{Mn}(\text{bpy}-\text{R})(\text{CO})_3\text{Br}]$ Complexes. *Chemistry – A European Journal* **2017**, *23* (20), 4782-4793.
9. Kokkes, M. W.; De Lange, W. G.; Stufkens, D. J.; Oskam, A., Photochemistry of metal–metal bonded complexes: III. MLCT photolysis of $(\text{CO})_5\text{MM}'(\text{CO})_3(\alpha\text{-diimine})(\text{M}, \text{M}' = \text{Mn, Re})$ in 2-Me-THF and THF at 293 K; Evidence of photocatalytic formation of $[(\text{Mn}(\text{CO})_3(\alpha\text{-diimine})(\text{P}(\text{n-Bu})_3)]^+[\text{M}(\text{CO})_5]^-$ upon photolysis in the presence of $\text{P}(\text{n-Bu})_3$. *Journal of Organometallic Chemistry* **1985**, *294* (1), 59-73.